J Membrane Biol (2010) 233:73–83
DOI 10.1007/s00232-010-9226-9

Long-Term Adaptation of *Bacillus subtilis* 168 to Extreme pH Affects Chemical and Physical Properties of the Cellular Membrane

Denisa Petrackova · Jaroslav Vecer · Jaroslava Svobodova · Petr Herman

Received: 29 September 2009 / Accepted: 8 January 2010 / Published online: 5 February 2010

Abstract We characterized physical and chemical properties of cell-membrane fragments from *Bacillus subtilis* 168 (trpC2) grown at pH 5.0, 7.0 and 8.5. Effects of long-term bacterial adaptation reflected in growth rates and in changes of the membrane lipid composition were correlated with lipid order and dynamics using time-resolved fluorescence anisotropy of 1,6-diphenyl-1,3,5-hexatriene. We demonstrate that the pH adaptation results in a modification of a fatty acid content of cellular membranes that significantly influences both the lipid-chain order and dynamics. For cultivation at acidic conditions, the lipid order increases and membrane dynamics decreases compared to pH 7.0. This results in rigid and ordered membranes. Cultivation at pH 8.5 causes slight membrane disordering. Instant pH changes induce qualitatively similar but smaller effects. Proton flux measurements performed on intact cells adapted to both pH 5.0 and 8.5 revealed lower cell-membrane permeability compared to bacteria cultivated at pH optimum. Our results indicate that both acidic and alkalic pH stress represent a permanent challenge for *B. subtilis* to keep a functional membrane state. The documented adaptation-induced adjustments of membrane properties could be an important part of mechanisms maintaining an optimal intracellular pH at a wide range of extracellular proton concentrations.

D. Petrackova · J. Svobodova
Department of Genetics and Microbiology, Faculty of Sciences, Charles University, Vinicna 5, 128 44 Prague 2, Czech Republic

J. Vecer · P. Herman (✉)
Faculty of Mathematics and Physics, Institute of Physics, Charles University, Ke Karlovu 5, 121 16 Prague 2, Czech Republic
e-mail: herman@karlov.mff.cuni.cz

Keywords Time-resolved fluorescence · Fluorescence anisotropy · Depolarization · Lipid order · DPH · pH stress · Lipid dynamics · Fatty acid profile · Proton permeability

Introduction

The gram-positive bacterium *Bacillus subtilis* inhabits the upper layer of the soil as its primary habitat. Within this ecosystem the bacteria experience a wide variety of environmental challenges as well as nutrient limitations that trigger adaptation mechanisms that allow them to survive under changed conditions. The cellular membrane is known to be the first barrier separating the cell interior from the extrinsic physical and chemical stress factors. Maintenance of cell integrity and cytoplasmic membrane integrity plays, therefore, a crucial role in preserving the cell viability and their metabolic functions. Cellular membranes modulate stress-signal transduction, and a molecular machinery triggering adaptation responses resides on the membrane as well (Poolman et al. 2002, 2004). It also constitutes a barrier against free passing protons and other ions. Physical properties of the lipid bilayer are therefore of particular importance and should be maintained in a narrow optimal range to ensure its full functionality (Mansilla et al. 2004; McElhaney and Souza 1976). These static and dynamic membrane properties, often covered by the broad and inaccurate term "fluidity," are tightly linked to the membrane composition and depend on lipid shape, interactions, packing, phase transition, dynamics, protein content and a number of related parameters (Denich et al. 2003; Mykytczuk et al. 2007). Membrane adaptation therefore results in readjustment of the membrane properties that restores the optimal

membrane state and compensates for perturbations caused by the extrinsic factors. This can happen in response to variations in temperature (Hazel 1995; Herman et al. 1994, 1998), pressure, ion concentrations, pH, availability of nutrients and xenobiotics.

Lipids are one of few classes of molecules that can adjust to environmental disturbances by changing their structure and relative fraction in response to variations in extracellular conditions (see, e.g., Denich et al. 2003, for review). The most extensively studied external factor stimulating adaptation of cellular membranes is temperature. Temperature variations cause significant changes of membrane properties that are compensated on a physiological level by an adjustment of membrane lipids (see, e.g., Hazel 1995, for review). Much less is known about the physical effects of pH on properties and adaptation of biomembranes. Surprisingly, no universal paradigm of preferred fatty acid (FA) membrane content was observed in bacteria treated by low pH. *Streptococcus mutans*, an etiological agent in human dental caries, displayed a shift from the short-chained saturated membrane FA (C14:0, C16:0) seen at pH optimum to the long-chained monounsaturated FA (C18:1 and C20:1) at pH 5 (Fozo and Quivey 2004). A similar response was detected in the membranes of oral bacteria *Lactobacillus casei* (Fozo et al. 2004). Such changes are usually accompanied by membrane fluidization. In contrast, log-phase *Listeria monocytogenes*, the causative agent of foodborne listeriosis, significantly increased the membrane content of straight-chain FA (C14:0 and C16:0) when adapted to pH 5.5 at the expense of decreased levels of C18:0 (van Schaik et al. 1999). Similarly, *Escherichia coli* O157:H7, a foodborne pathogen persisting in acidic foods, increased an amount of C16:0 palmitic acid when exposed to pH 5. A fraction of *cis*-vaccenic acid (C18:1ω7c) in the cell membranes decreased (Yuk and Marshall 2004). This would be usually interpreted as membrane rigidization. Detailed mechanisms relating highly variable and often opposite chemical responses to a functional membrane state have not been identified yet.

Proton permeability is an important factor permitting cells to maintain the proton motive force for vital energy-transducing processes. It has been shown that the proton permeability correlates with the physical state of the lysosomal membrane; in particular, the permeability increases with increasing membrane fluidity (van de Vossenberg et al. 1999a; Wan et al. 2002; Zhang et al. 2000). The proton permeability of liposomes made from cellular membrane lipids extracted from *B. subtilis* grown at different temperatures was shown to be almost constant when measured at growth temperature. The growth temperature–dependent lipid variation therefore permits maintenance of the proton permeability of the cytoplasmic membrane (the "homeo-proton permeability" concept) (van de Vossenberg et al. 1999a). Recently, effects of acid shock on the lactic acid bacterium *Oenococcus oeni* were investigated (Chu-Ky et al. 2005). The shocks were shown to induce a rigidifying effect on the cell membranes without affecting cell viability. Acid-adapted *E. coli* cells were shown to better withstand extremely acidic pH in simulated gastric fluids (pH 1.5) than nonadapted cells. The longer survival correlated with lower cell membrane fluidity caused by an adaptation-induced exchange of membrane lipids (Yuk and Marshall 2004, 2005). On the other hand, environmental pH affected neither the membrane structure nor the permeability of halo(alkali)philic archaeal membranes (van de Vossenberg et al. 1999b). The proton permeability of the liposomes formed from lipids of halophiles was essentially constant when measured at pH between 7 and 9.

It has been demonstrated that the lipid and FA composition of the *B. subtilis* cellular membrane is responsive to environmental stress, e.g., temperature (Svobodova et al. 1988; van de Vossenberg et al. 1999a). The FA profile of gram-positive *B. subtilis* was shown to be dominated by the iso- and anteiso-branched FAs that are synthesized from branched amino acid precursors (Clejan et al. 1986). Since the melting temperature of anteiso-branched FAs is significantly lower than that for the iso-branched isomers, variation of their relative fraction is one of the important factors contributing to adjustment of membrane phase transition and, consequently, a physiologically optimal membrane state (Kaneda 1977, 1991).

Spectral and chemical properties of popular membrane probe 1,6-diphenyl-1,3,5-hexatriene (DPH) are ideally suited for investigation of membrane structure (Shinitzky and Barenholz 1978). This highly hydrophobic molecule that is essentially nonfluorescent in aqueous solution incorporates spontaneously into the hydrophobic core of the membrane with an accompanying dramatic increase of the fluorescence quantum yield. The cylindrical rod-like shape of the molecule allows its parallel orientation to the FA side-chains that restrict rotational freedom of the probe's long axis (Trevors 2003). Changes of the FA chain dynamics and order therefore propagate to the orientational distribution of DPH that can be accessed by time-resolved fluorescence anisotropy.

Time-resolved fluorescence anisotropy measurements are highly suitable for evaluation of rotational diffusion of fluorescent probes in membranes (Lakowicz 1999). Unlike the steady-state approach, polarized time-resolved experiments yield deeper insight into the origin of the membrane adaptation by differentiating between changes of the probe fluorescence lifetime that sensitively reflect adaptation-induced variation of the probe microenvironment from rotational diffusion of the probe inside the membrane. The rotational diffusion of the probe is affected by its interactions

with lipid chains that modulate both the rotational diffusion rate and the extent of the rotational motion that is influenced by a packing of the lipid chains (lipid order) (Jahnig 1979; Kinosita et al. 1977; van der Meer et al. 1984). All this information can be extracted from a detailed shape of the fluorescence anisotropy decay, $r(t)$ (Herman et al. 1994). It is evident that the time-resolved approach offers a significant advantage over simple and highly popular steady-state fluorescence anisotropy measurements where the emission lifetime (τ) and diffusion information (ϕ) are intermingled into a single scalar value as described by the Perrin equation (Lakowicz 1999): $r_s = r_0/(1 + \tau/\phi)$. The measured steady-state anisotropy, r_s, depends on the fluorescence lifetime of the probe used. If the lifetime varies, e.g., by influence of temperature or other external factors, the anisotropy exhibits variations that are not relevant to changes of the membrane state. The time-resolved fluorescence approach eliminates such possible bias caused by the fluorescent probe itself and yields true membrane-related information.

In order to shed more light on the effects of long-term pH adaptation of *B. subtilis* in the context of membrane structure modifications, we focused on adaptation-induced alterations of membrane lipid composition. Accompanying changes of physical membrane properties, in particular, an adjustment of membrane lipid order and lipid-chain dynamics was characterized by time-resolved fluorescence spectroscopy and DPH fluorescence probe. Effects of abrupt pH changes on the physical properties of the pH-adapted membranes and adaptation-induced modulation of membrane permeabilities were comparatively evaluated as well.

Materials and Methods

Cultivation of Bacteria

The bacterial strain *B. subtilis* 168 (trpC2) (wild-type, laboratory stock) was used for all experiments. The strain was maintained on a slate agar (nutritive medium 2; Imuna, Sarisske Michalany, Slovak Republic). The bacteria were routinely grown under vigorous agitation (200 rpm) in an orbital shaker in the fluid complex medium with 0.15% (w/v) Bacto beef extract (GIBCO, Invitrogen, Carlsbad, CA), 0.15% (w/v) yeast extract (GIBCO), 60 mM NaCl (Imuna), 20 mM K_2HPO_4 (Fluka, Buchs, Switzerland), 10 mM KH_2PO_4 (Fluka), 0.5% bactopeptone (Oxoid, Basingstoke, UK) and 0.5% glucose. The cultivation was done at pH 5.0, 7.0 or 8.5.

Cultures of *B. subtilis* were inoculated from cultures grown overnight and cultivated on slant agar by propagation of the cells on the complex medium of the appropriate pH. Then, cells were grown at 40°C and growth was monitored by measurements of optical density at 420 nm (OD_{420}). Cells were harvested by rapid filtration when the culture reached an OD_{420} of 0.6 (a mid-exponential phase). Long-term adaptation was accomplished by keeping cells on the slant agar at the specific pH for 20 h. Short-term adaptation was done by changing the pH value of the cultivation medium to 5.0 or 8.5 for 15 min before cell harvesting. Then, cells were used for the isolation of plasma membranes. During cultivation, the bacteria exhibited a tendency to acidify the cultivation medium. The pH value was therefore continuously monitored and adjusted by a stepwise addition of 500 mM KOH, if necessary. Acidification was especially pronounced during cultivation at pH 8.5.

Membrane Isolation

Bacteria were harvested by filtration through the Pragopor 5 filter (pore size 0.6 μm; Pragochema, Prague, Czech Republic), washed with a phosphate buffer (50 mM, pH 8.0) and resuspended in the same buffer. Cells were disrupted by the enzymatic method using lysozyme, deoxyribonuclease 1 and ribonuclease at final concentration of 300, 10 and 10 μg/ml, respectively (Bisschop and Konings 1976). Additionally, the protease inhibitor phenylmethylsulphonyl fluoride (PMSF), at a final concentration of 0.5 mM, was added to the suspension; and cells were incubated for 30 min at 40°C in a shaker. Then, membrane fractions were separated by ultracentrifugation (20,000×*g*, 60 min, 4°C). The protein concentration of the pellet (the membrane fraction) was determined with the commercial BCA Protein Assay kit (Pierce, Rockford, IL). The membranes were stored as frozen aliquots at −75°C.

Lipid Isolation

For lipid extraction we used the hexane and isopropanol extraction method of Radin (1981). The method was modified for its application to the bacterial material. The mid-exponential cells harvested from about 1,000–1,500 ml of culture were resuspended in 100 ml of the extract solution (hexane and isopropanol, 3:2 v/v) and incubated overnight under mild shaking at 4°C. Then, cells were separated by centrifugation (4,300×*g*, 10 min, 0°C). The supernatant was removed and evaporated in a rotational vacuum evaporator thermostated to 40°C. The resulting lipid fraction was solubilized into 50 ml of chloroform and filtered, and the solvent was gently evaporated. The isolated lipids were stored at –75°C.

FA Analysis

FA profiles of *B. subtilis* were determined from about 1 mg of the isolated lipids. To determine the FA composition,

methyl esters were prepared from isolated phospholipids by *trans*-esterification with sodium methoxide and HCl in methanol (Glass 1971). The methyl esters were analyzed using a Varian (Palo Alto, CA) 3400 gas chromatography system coupled to a Finnigan INCOS 50 mass spectrometer (San Jose, CA) equipped with a DB5 column and ProLab Resources (Madison, WI) software. A mixture of bacterial FA methyl esters (Supelco) was used as standard.

Cell Membrane Labeling

Membrane suspensions were diluted in the phosphate buffer (50 mM; pH 5.0, 7.0 or 8.5) typically to the concentration of 90 μg/ml of membrane protein. A DPH solution (3 mM) in acetone was diluted (1:1,000 v/v) in a vigorously stirred membrane suspension. The labeled suspension was incubated for 30 min at 25°C before fluorescence measurements.

Time-Resolved Fluorescence Measurements

Fluorescence emission and anisotropy decays were measured on an apparatus comprised of a pulsed excitation source and time-correlated single photon counting detection with a cooled MCP-PMT (Hamamatsu, Shizuoka, Japan; R3809U-50). For the excitation of DPH fluorescence we used a picosecond cavity-dumped dye laser (Spectra Physics, Mountain View, CA; model 375) emitting at 710 nm. The laser output at repetition frequency of 4 MHz was frequency-doubled to 355 nm and used for excitation. DPH fluorescence was collected through monochromator at 430 nm (slit width 15 nm). A supplemental absorption long-pass filter with the cut-off wavelength of 405 nm was placed in front of the input slit to enhance suppression of scattered light. The timescale of 36 ps/channel was used for all measurements. Typically, we used 1,024 channels per decay and data were accumulated until the peak count of 10^5 was reached. Intensity decays were acquired under the "magic angle" conditions when the measured intensity decay, $I(t)$, is unbiased by the rotational diffusion of the chromophore. In the fluorescence anisotropy experiments the polarized components $I_{||}(t)$ and $I_{\perp}(t)$ were accumulated quasi-simultaneously with a switching frequency of 15 s. The polarized decays were measured with the emission polarizer set in the fixed vertical position while the polarization plane of the excitation beam was switched between 0 and 90°, respectively. In this configuration the G-factor was close to unity, and its exact value was determined in a separate experiment. The apparatus response function was measured using diluted Ludox solution. Samples were placed in a thermostatic holder and measured at 22°C. All experiments were repeated with an aliquot of an unlabeled sample in order to evaluate background emission. This background was always lower than 3% of the total intensity and subtracted from decays of the labeled samples before data analysis.

Data Analysis

Fluorescence intensity was assumed to decay multiexponentially according to the formula

$$I(t) = \sum_i \alpha_i \cdot e^{-t/\tau_i} \tag{1}$$

where τ_i are fluorescence lifetime components and α_i are corresponding amplitudes. The mean lifetime was calculated as

$$\tau_{\text{mean}} = \sum_i f_i \tau_i \tag{2}$$

where f_i is the intensity fraction of the i-th lifetime component.

$$f_i = \alpha_i \tau_i / \sum_i \alpha_i \tau_i \tag{3}$$

Fluorescence anisotropy decays, $r(t)$, can be constructed from the parallel $I_{||}(t)$ and the perpendicular $I_{\perp}(t)$ decay components according to the formula

$$r(t) = \frac{I_{||}(t) - I_{\perp}(t)}{I(t)} = \frac{I_{||}(t) - I_{\perp}(t)}{I_{||}(t) + 2I_{\perp}(t)} \tag{4}$$

Because $r(t)$ is distorted by a convolution of $I_{||}(t)$ and $I_{\perp}(t)$ with the excitation pulse and the fluorescence anisotropy cannot be directly deconvolved, it is advantageous to rearrange Eq. 4 and directly deconvolve $I_{||}(t)$ and $I_{\perp}(t)$(Cross and Fleming 1984; Tao 1969):

$$\begin{aligned} I_{||}(t) &= \frac{I(t)}{3} \cdot [1 + 2r(t)] \\ I_{\perp}(t) &= \frac{I(t)}{3} \cdot [1 - r(t)] \end{aligned} \tag{5}$$

We used global simultaneous analysis of $I_{||}(t)$ and $I_{\perp}(t)$ to increase the accuracy of the extracted $r(t)$ (Beechem et al. 1985; Knutson et al. 1983). The time-dependent anisotropy $r(t)$ in Eq. 5 was assumed to decay multiexponentially:

$$r(t) = \sum_i \beta_i e^{-t/\phi_i} + r_\infty \tag{6}$$

where ϕ_i are rotational correlation times and β_i are corresponding amplitudes. We can write:

$$\sum_i \beta_i + r_\infty = r_0 \tag{7}$$

where r_0 is a zero-time anisotropy at $t = 0$ s. This constant is characteristic for the probe used and does not depend on

membrane properties. The limiting anisotropy r_∞, characterizing rotational freedom of the probe in the membrane, can be expressed as follows (Jahnig 1979; Kinosita et al. 1977; Lipari and Szabo 1980; Zannoni 1981):

$$r_\infty = r_0 \cdot <P_2>^2 \quad (8)$$

where $<P_2>$ is the second-rank order parameter. Mean correlation time, ϕ_{mean}, was calculated as follows:

$$\phi_{\text{mean}} = \sum_i \beta_i \phi_i / \sum_i \beta_i \quad (9)$$

Proton Flux Assay

Proton flux measurements were performed according to a modified method of Jordan et al. (1999). Briefly, pH-adapted cells in exponential growth phase were harvested, thoroughly washed by 100 mM KCl and resuspended in 10 ml of the same unbuffered solution. Final concentration of the cells in the suspension was always kept at 25 mg/ml (wet weight). Then, the suspension was incubated at 30°C with continuous stirring until pH stabilized near the neutral value (3–4 min). When necessary, the pH was adjusted by a small amount of KOH. Then, the suspension was pulse-perturbed by addition of 50 µl of 0.5 M HCl and pH drifts were monitored for about 10 min. The initial abrupt acidification of the medium was followed by a slow pH increase caused by proton influx to the cytoplasm. The rate of proton accumulation was qualitatively estimated from the initial slope of the pH increase.

Results and Discussion

Growth of *B. subtilis* 168 trp2- in the Complex Medium of Different pH

We compared bacterial growth rates of cells adapted to extreme pH. Bacteria were adapted to pH 5.0 and 8.5 by growing them on slant agar for 16 h at 40°C. Then, cells were inoculated into the liquid complex medium of the same pH and growth curves were measured. Because the cultures typically reached the early stationary phase in 20 h, the bacteria were supposed to be already pH-adapted. Control experiments were performed by growing the cells in the complex medium of pH 7.0. Measured growth rates, calculated as $c = \Delta\log_2(OD_{420})/\Delta t$, are depicted in Fig. 1. It is seen that the pH adaptation does not allow a full recovery of the growth rates measured under optimal growth conditions (pH 7.0, 40°C). Compared to pH 7.0, where $c = 0.055\ \text{min}^{-1}$, the growth rate reduced to $0.037\ \text{min}^{-1}$ and $0.032\ \text{min}^{-1}$ for bacteria adapted to pH 5.0 and 8.5, respectively. The doubling time correspondingly increased

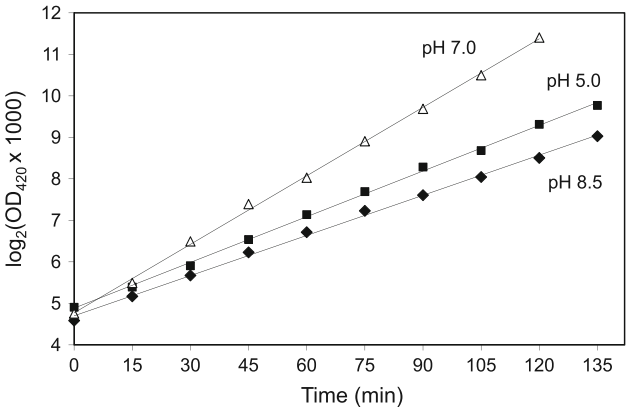

Fig. 1 Growth curves of *B. subtilis* after the long-term adaptation to pH 5.0 (*filed square*) and pH 8.5 (*filled diamond*). The control growth curve at pH 7.0 is depicted by open symbols (*open triangle*). *B. subtilis* 168 trp2- was grown for 16 h on slant agar at pH 5.0, 8.5 and 7.0 (control). Then, cells were transferred to the complex cultivation medium of the same pH for measurements of growth rates. Rates were $0.055\ \text{min}^{-1}$ (doubling time $T = 18$ min), $0.037\ \text{min}^{-1}$ ($T = 27$ min) and $0.032\ \text{min}^{-1}$ ($T = 31$ min) at pH 7.0, 5.5 and 8.5, respectively. All measurements were done under good aeration at 40°C. Growth curves represent an average of typically six independent experiments

from 18 min to 27 and 31 min at acidic and basic pH, respectively. The 8% lower increase of the doubling time per pH unit measured for cells adapted to pH 5.0 compared to cells adapted to pH 8.5 could indicate that the compensation mechanisms work more efficiently for acidic than for basic pH shifts.

FA Profiles of *B. subtilis* Cells Cultivated at pH 5.0 and 8.5

In order to determine to what extent the long-term environmental pH stress influences lipid composition of the cellular membranes, we characterized the FA profile synthesized by *B. subtilis* under different growth conditions. Figure 2 shows the distribution of 13 main FA species of *B. subtilis* in membranes of bacteria grown at pH 5.0 (BS50), pH 8.5 (BS85) and the control pH 7.0 (BS70). It can be seen that under optimal pH conditions the FA profiles of BS70 contain more than 80% of the iso- and anteiso-branched FA (Fig. 2c). The profile is dominated by i-15:0, a-15:0, i-17:0 and a-17:0 FAs (Fig. 2a, b). This FA composition is typical for the *B. subtilis* strain 168 (Clejan et al. 1986). Compared to BS70, the lipid profile of BS50 exhibits a marked increase in the shorter iso-branched FA with an even number of carbons, i-14:0 and i-16:0. This increase was at the expense of a decreased content of the longer iso-branched FAs with an odd number of carbons, i-15:0 and i-17:0 (Fig. 2a). Specifically, the fractional ratio of (i-C:14 + i-C:16)/(i-C:15 + i-C:17) increased from 0.25 in BS70 to 1.3 in BS50 membranes. The summary presented in Fig. 2c suggests that the total content of the

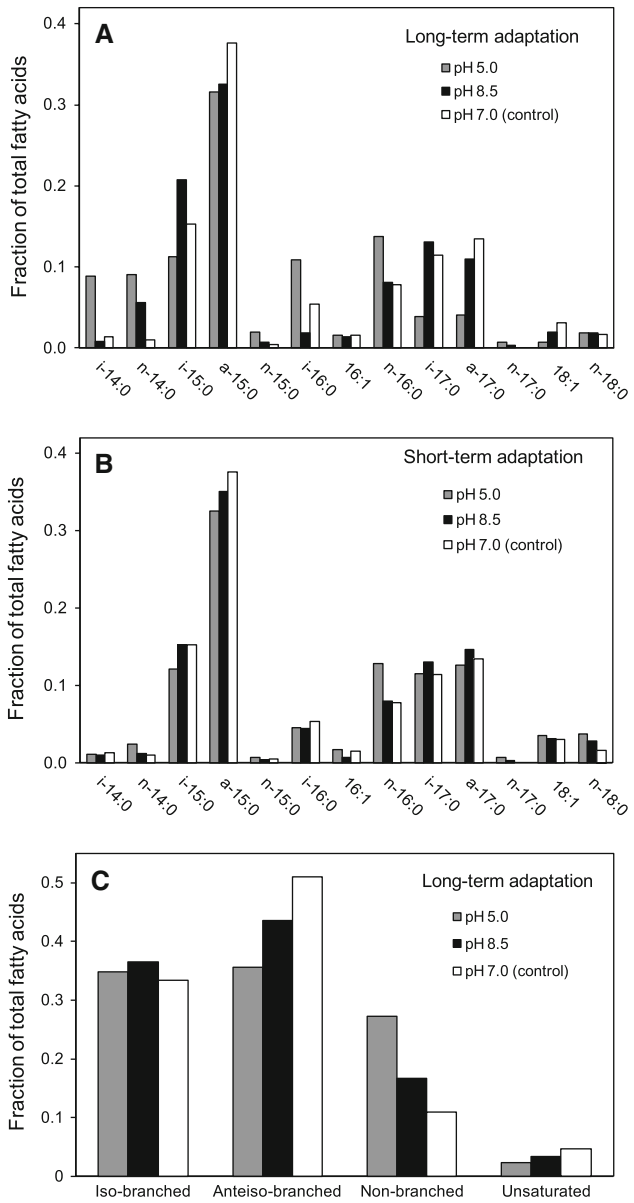

Fig. 2 Effect of pH on FA profiles of cell membranes from *B. subtilis*. Fractional contributions of dominating FA species after long-term (**a**) and short-term (**b**) adaptation to pH 5.0 and 8.5. **c** Fractions of the main structural FA types after long-term adaptation. Control FA profiles for cells cultivated at pH 7.0 are presented for comparison. *i-*, *a-* and *n-* represent branching patterns of iso-, anteiso- and nonbranched FAs, respectively. Accuracy of the individual FA determination is about 15%

iso-branched FA of BS50 is similar to that of the control membranes BS70. At the same time, the sum of non-branched saturated FA increases at the expense of the anteiso-FA series. The level of straight-chain n-14:0, 15:0 and 16:0 also increases. Due to a lower melting temperature of the anteiso-branched FAs compared to the iso-branched isomers (Gurr et al. 2002), our result can be interpreted as a "thermodynamic rigidization" of membranes isolated from bacteria cultivated at acidic pH.

Figure 2a shows that the FA profile of BS85 resembles more closely the profile of the BS70 control membranes. We found decreases of a-15:0 and a-17:0 FAs as well as of the iso-branched FA i-16:0. This decrease was compensated by an increase of i-15:0 together with an increase of nonbranched 14:0 FA. Interestingly, the fractional ratio of (i-C:14 + i-C:16)/(i-C:15 + i-C:17) exhibited the opposite trend compared to acidic conditions and decreased from 0.25 in BS70 to 0.08 in BS85 membranes. This indicates a higher content of the longer iso-branched FAs. The summary in Fig. 2c exhibits smaller adaptation-induced differences of BS85 than the acid-adapted BS50 membranes. The conclusion is consistent with the lowest growth rate of bacteria adapted to pH 8.5 (Fig. 1).

We also examined a short-term pH adaptation in order to see which FA class first responds to the changed pH conditions. Figure 2b demonstrates changes in the FA profiles after 15-min incubation at the stress pH. From visual comparison of Fig. 2b and 2a it can be seen that the readjustment of a-15:0 and n-16:0 is almost completed within the first 15 min. These FAs are therefore responsible for the early membrane adaptation to changed pH conditions leading to the rigidization of the plasma membranes. The content of the other FAs is adjusted later during the adaptation process. Our observation is in agreement with the literature since similar rapid adaptation of the FA content in the plasma membrane of *B. subtilis* was observed during a cold shock (Suutari and Laakso 1992; Svobodova et al. 1988). It was reported that within 20 min from the onset of the cold stress the major branched FAs were replaced by straight-chain ones. Synthesis of low melting unsaturated FA was reported to be induced within this short time period as well.

Time-Resolved Fluorescence Measurements

In order to evaluate to what extent the observed changes in the membrane composition influence their physical properties, we performed a series of time-resolved fluorescence experiments with DPH fluorescence probe. An example of experimental data is presented in Fig. 3. Visual inspection of the figure reveals that both the fluorescence (Fig. 3a) and the anisotropy decays (Fig. 3b) acquired on pH-adapted membranes at a corresponding cultivation pH significantly differ. This observation indicates that both the chemical microenvironment of DPH that influences emission decay rates and membrane packing reflected by the anisotropy decays are different in membranes adapted to different pH.

Fluorescence decays of DPH in membranes were found to be biexponential under all experimental conditions. The biexponential decays observed in membranes of *B. subtilis* are in accord with typical characteristics of DPH fluorescence in solutions as well as in other membrane systems and reflect the complex nature of DPH photophysics (Herman

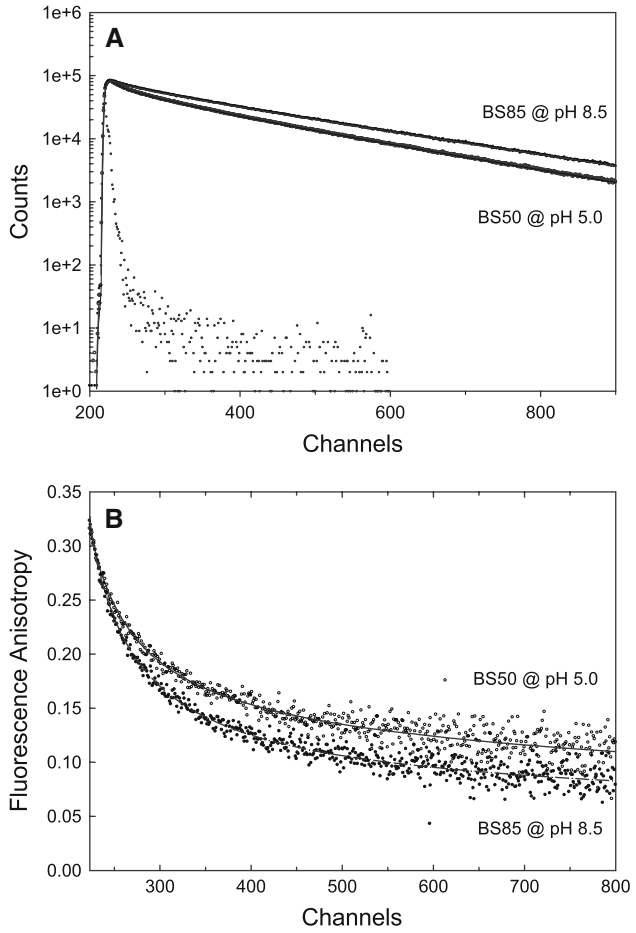

Fig. 3 Fluorescence emission (**a**) and anisotropy (**b**) decays of DPH in membranes from *B. subtilis* cultivated at pH 5.0 and 8.5. Measurements were performed at pH of the cultivation

et al. 1994). Detailed dependence of mean fluorescence lifetimes, τ_{mean}, on the cultivation and measurement pH is summarized in Table 1 and Fig. 4. It can be seen that an adaptation-induced FA exchange significantly influences membrane properties since at any measurement pH τ_{mean} increases with increasing cultivation pH. Such an observation is consistent with a modulation of the DPH microenvironment resulting from membrane adaptation. From Fig. 4 we can see that lifetime changes caused by variation of the environmental pH are almost insignificant, especially for BS50 and BS70 membranes. A small lifetime increase was recorded on BS85 membranes at basic pH. We suggest that the effect could indicate a loosened structure of BS85 resulting in a higher sensitivity of DPH fluorescence to quenching by protons.

Order Parameters

To evaluate structural membrane changes caused by long-term adaptation of *B. subtilis* to extreme pH values as well

Table 1 Summary of fluorescence emission and anisotropy decay parameters of DPH embedded in plasma membranes from *B. subtilis* cultivated at different pH

Cult.	Measurement pH 5.0							Measurement pH 7.0							Measurement pH 8.5						
	τ_{mean} (ns)	β_1	ϕ_1 (ns)	β_2	ϕ_2 (ns)	r_∞	ϕ_{mean} (ns)[a]	τ_{mean} (ns)	β_1	ϕ_1 (ns)	β_2	ϕ_2 (ns)	r_∞	ϕ_{mean} (ns)[a]	τ_{mean} (ns)	β_1	ϕ_1 (ns)	β_2	ϕ_2 (ns)	r_∞	ϕ_{mean} (ns)[a]
pH 5.0	7.2	0.099	1.1	0.117	7.4	0.105	4.5	7.2	0.119	1.1	0.110	6.7	0.094	4.4	7.2	0.105	0.8	0.128	4.8	0.095	4.7
pH 7.0	7.6	0.086	1.0	0.137	6.6	0.092	3.8	7.7	0.113	1.1	0.122	6.1	0.083	3.7	7.5	0.125	1.1	0.125	6.3	0.073	4.3
pH 8.5	7.8	0.096	1.1	0.136	7.3	0.087	3.0	7.9	0.126	1.2	0.122	7.6	0.077	3.7	8.3	0.124	1.1	0.126	6.5	0.078	3.8

[a] Mean correlation time values were calculated according to Eq. 9

as an immediate lipid reordering caused by extracellular pH variations, we performed time-resolved fluorescence anisotropy measurements. Membranes BS50, BS70 and BS85 were measured at pH 5.0, 7.0 and 8.5, respectively. Then, the order parameter $<P_2>$, reflecting the lipid chain order and the rotational correlation time of DPH in membranes, was evaluated. Results of this grid experiment are summarized in Table 1 and Fig. 5.

The $<P_2>$ order parameters calculated from the limiting anisotropy r_∞ according to Eq. 8 depend on a local angular distribution $P_{eq}(\theta)$ of the probe molecule within the lipid bilayer according to the formula (van der Meer et al. 1984):

$$<P_2> = \int_0^\pi P_{22}(\cos(\theta))P_{eq}(\theta)\sin(\theta)d\theta \qquad (10)$$

where $P_{22}(\theta)$ is a Legendre polynomial and θ is an angle between the local director in the membrane and the long axis of DPH. Since the order of lipid chains determines $P_{eq}(\theta)$ of the probe, $<P_2>$ describes this order as well. For fully ordered membranes, all DPH molecules are aligned with the local director in the membrane ($\theta = 0°$) and $<P_2> = 1$. For complete disorder, all orientations of DPH are possible and $<P_2> = 0$. Interpretation of r_∞ can be done also in the frame of a "cone model," where the probe freely wobbles in a cone with a semiangle θ (Kinosita et al. 1977): $r_\infty = r_0 \cdot [1/2\cos(\theta)(1+\cos(\theta)]^2$. Since the probe rotation is restricted by FA chains, θ reflects a degree of the lipid order (packing). The larger the lipid disorder, the wider the cone that DPH can explore during its rotational diffusion. As a consequence, r_∞ decreases. Looking along the diagonal of Fig. 5a we can clearly see that the membrane adaptation results in a substantially different lipid chain order, membranes adapted to the acidic pH being the most ordered. We can also see that as the cultivation pH increases, all membranes disorder. The effect is independent of the measurement pH, and the difference is especially visible when BS50 and BS70 membranes are compared. Similar lipid disordering can be seen when the measurement pH for any of the BS50, BS70 and BS85

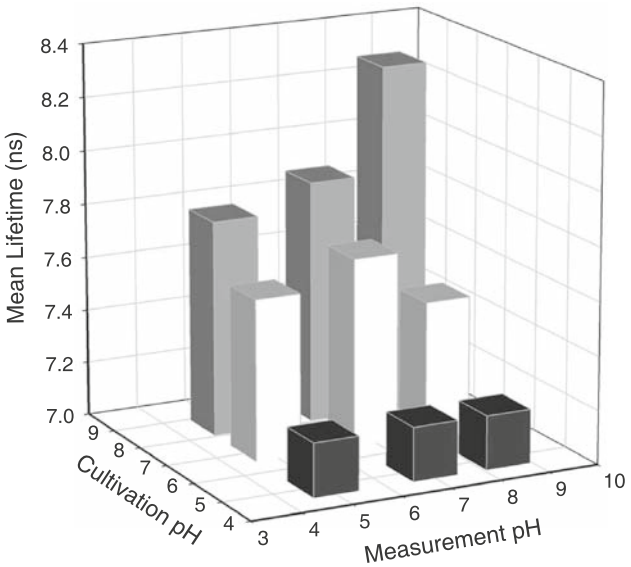

Fig. 4 Mean fluorescence lifetime of DPH in BS50 (*black bars*), BS70 (*white bars*) and BS85 (*gray bars*) membranes as a function of measurement pH. Standard deviation is 0.05 ns

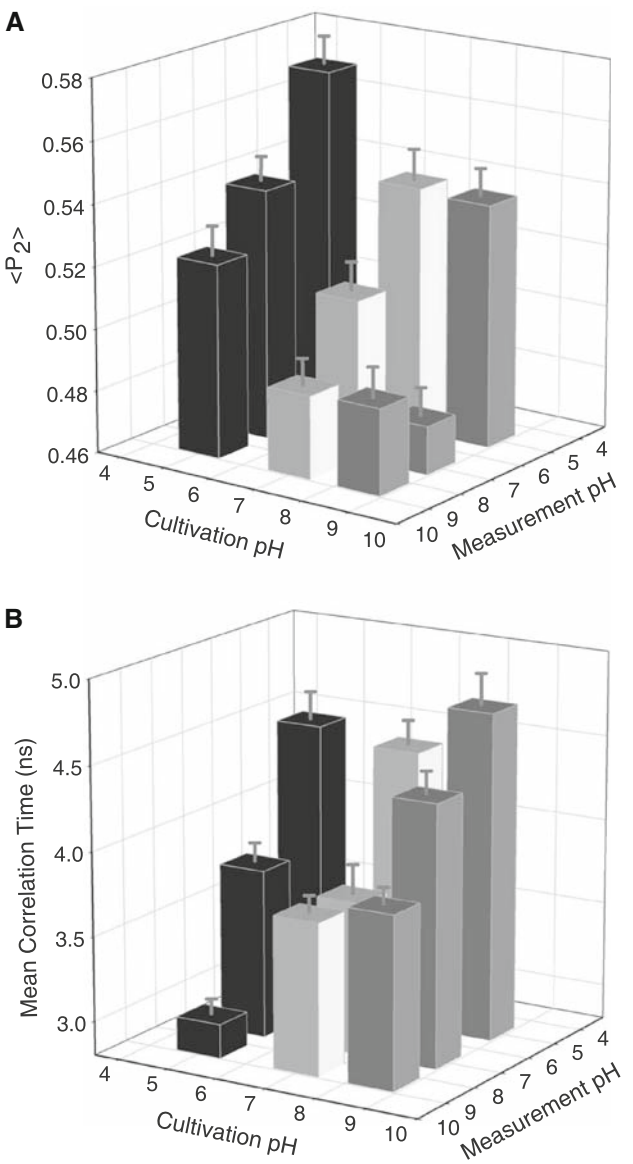

Fig. 5 Overview of time-resolved fluorescence anisotropy results. **a** Second-rank order parameters $<P_2>$ of DPH in BS50 (*black bars*), BS70 (*white bars*) and BS85 (*gray bars*) membranes as a function of measurement pH. Order parameters were calculated from data in Table 1 using equations 7 and 8. **b** Mean correlation time of DPH in BS50 (*black bars*), BS70 (*white bars*) and BS85 (*gray bars*) membranes as a function of measurement pH. Error bars were estimated from three to five measurements made on two membrane preparations

cultivations increases. Taking into account data uncertainty, the qualitative behavior of all membrane cultivations was the same. The membrane ordering seems to be important for modulation of proton permeability and the ability of cells to maintain mostly invariant intracellular pH under a wide variety of environmental conditions. Importantly, as seen from Fig. 5a, changing the environmental pH always causes a fast preadaptation response, resulting in the FA-chain reordering that partially offsets the environmental stress. Later, a slower adaptive FA exchange facilitates further membrane reordering.

Lipid Chain Dynamics

Rotational correlation times of DPH within the BS50, BS70 and BS85 membranes at various pH values are presented in Table 1. It can be seen that two correlation time components were resolved in the anisotropy decays under all conditions. The correlation times are inversely proportional to rotational diffusion rates and reflect the dynamics of the probe reorientation. The longer the correlation time, the slower the rotational movement of DPH modulated by interactions of the probe with lipid chains. Since DPH is a rod-like molecule, it exhibits several rotational diffusion rates along different molecular axes (Lakowicz 1999). Moreover, biological membranes are not uniform lipid bilayers. The current view of membrane organization includes the existence of dynamic lipid microdomains/rafts that participate in diverse cellular functions such as regulation of cellular polarity, cellular signaling and adhesion (Dupree and Pomicter 2009; Fullekrug and Simons 2004; Goni et al. 2008). As a consequence, the physical properties of membranes can differ at different membrane locations. The heterogeneity of the fluorescence anisotropy decays is therefore not surprising. Due to the rather complicated interpretation of the individual correlation time components, we preferred to characterize the rotational diffusion of DPH by a single ϕ_{mean}, which was calculated from values given in Table 1 using Eq. 9. These mean values are plotted in Fig. 5b and represent a qualitative indicator of DPH dynamics within the membranes. In turn, ϕ_{mean} reflects the internal membrane dynamics since the DPH reorientational rate depends on the collisional rate of the probe with lipid chains. Inspection of Fig. 5b reveals that both the cultivation and the measurement pH affect ϕ_{mean} in all membrane cultivations. When we look along the measurement pH axis, we can see that ϕ_{mean} increases with decreasing measurement pH. This indicates a decrease of membrane dynamics. When we look along the cultivation pH axis, we notice the opposite tendency. Decrease of the cultivation pH causes decrease of ϕ_{mean}, which can be interpreted as increased lipid dynamics compensating for membrane rigidization caused by acidification of the environment. The compensation effect is clearly seen when BS50 membranes are shifted from pH 5.0 to 8.5 (black bars). Such alkalization of the environmental pH is accompanied by a significant decrease of ϕ_{mean} (increase of membrane dynamics). When the alkalization persists, adaptation mechanisms strive to reverse the change and the adaptive FA modification results in decreased membrane dynamics (increased ϕ_{mean}). The end point of the whole process can be traced on the diagonal of Fig. 5b (BS85 membranes at pH 8.5). We can conclude that the pH adaptation seems to maintain optimal membrane dynamics and to compensate for changes caused by a long-term deviation of environmental pH from the optimal value.

Proton Accumulation Rates

It is of great interest to evaluate how chemical and structural changes correlate with proton permeabilities of the membranes. Therefore, we performed an acidic pH-jump assay on intact cells adapted to pH 5.0, 7.0 and 8.5. Results are summarized in Fig. 6. It can be seen that following the initial pH pulse, the pH of the cell suspension starts to gradually increase as a consequence of cellular proton uptake. The rate of the pH increase was found to be the highest for *B. subtilis* cultivated at pH optimum. An analysis of the polynomial fits revealed that the initial rates of the pH increase (the first derivative at $t = 0$ s) are 0.08, 0.09 and 0.16 pH units/min for bacteria adapted to pH 5.0, 8.5 and 7.0, respectively. This indicates decreased proton permeability of the stress-adapted membranes. Similar

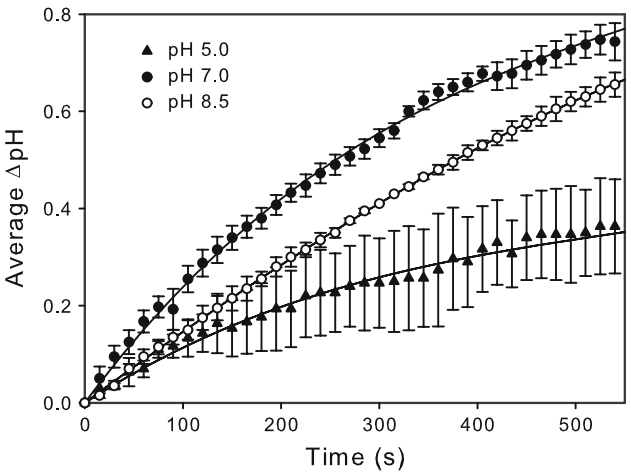

Fig. 6 Proton accumulation data measured on intact *B. subtilis* cells long-term-adapted to pH 5.0 (*filled triangle*), 7.0 (*open square*) and 8.5 (*open circle*). The ΔpH is change of cell-suspension pH after an acidic pH jump. *Symbols* represent a mean value of three to five measurements, and *solid lines* are polynomial fits. The pH increase of the medium is caused by cellular proton uptake. Initial rates of pH change (first derivative at $t = 0$ s) are 0.08, 0.09 and 0.16 pH units/min for bacteria adapted to pH 5.0, 8.5 and 7.0, respectively

coupling between membrane FA profiles of *B. subtilis* and H^+ membrane permeability that allows *B. subtilis* to sustain a proton motive force and survive at a wide range of growth temperatures has been reported (van de Vossenberg et al. 1999a). It has to be noted that the observed pH effects are caused by a net H^+ movement across the membrane. From our findings it is impossible to decide whether the lower permeability is caused by decreased proton influx or increased activity of H^+ pumps transporting protons out of the cytoplasm. In any case, our data reveal a strong correlation between structural and functional membrane properties that allows *B. subtilis* to survive highly unfavorable pH conditions.

Conclusion

Our data document that a change of cultivation conditions to both the acidic and basic pH triggers a physiological response that partially offsets the environmental stress. Long-term pH adaptation results in a modification of the FA content in cellular membranes and consequently in a change of physical membrane properties. We found that both the lipid-chain order and dynamics are under adaptive pH control. As the cultivation pH decreases, the lipid order increases. Compared to the BS70, membranes from bacteria cultivated at acidic pH are more rigid and ordered. Cultivation at pH 8.5 causes slight membrane disordering. Instant variation of the lipid order of the fully adapted membranes that were subjected to variation of external pH was observed to be qualitatively similar to the adaptation-induced changes. Their extent, however, was significantly smaller. The adaptation also seems to maintain optimal membrane dynamics perturbed by fluctuations of environmental pH. Interestingly, in both cases the adaptation to suboptimal pH conditions correlated with decreased net proton permeability of cellular membranes.

It was demonstrated earlier that the lipid order is directly related to the lateral pressure which is experienced by other membrane components (Fulford and Peel 1980). The lateral pressure decreases with increasing lipid order and modulates the activity of membrane enzymes (Amler et al. 1990; Owicki et al. 1978). Changing the lipid order and dynamics could therefore be a mechanism for adjustment of both passive cellular membrane permeability and regulation of the active proton transport in order to keep optimal intracellular pH at a wide range of extracellular proton concentrations.

Acknowledgements This work was supported by grant 129/2003 of the Grant Agency of Charles University in Prague and by research projects MSM0021620835 and MSM113100256 of the Ministry of Education, Youth and Sports of the Czech Republic.

References

Amler E, Jasinska R, Drahota Z, Zborowski J (1990) Membrane lateral pressure as a modulator of glycerol-3-phosphate dehydrogenase activity. FEBS Lett 271:165–168

Beechem JM, Ameloot M, Brand L (1985) Global and target analysis of complex decay phenomena. Anal Instrument 14:379–402

Bisschop A, Konings WN (1976) Reconstitution of reduced nicotinamide adenine dinucleotide oxidase activity with menadione in membrane vesicles from the menaquinone-deficient *Bacillus subtilis* aro D. Relation between electron transfer and active transport. Eur J Biochem 67:357–365

Chu-Ky S, Tourdot-Marechal R, Marechal PA, Guzzo J (2005) Combined cold, acid, ethanol shocks in *Oenococcus oeni*: effects on membrane fluidity and cell viability. Biochim Biophys Acta 1717:118–124

Clejan S, Krulwich TA, Mondrus KR, Seto-Young D (1986) Membrane lipid composition of obligately and facultatively alkalophilic strains of *Bacillus* spp. J Bacteriol 168:334–340

Cross AJ, Fleming GR (1984) Analysis of time-resolved fluorescence anisotropy decays. Biophys J 46:45–56

Denich TJ, Beaudette LA, Lee H, Trevors JT (2003) Effect of selected environmental and physico-chemical factors on bacterial cytoplasmic membranes. J Microbiol Methods 52:149–182

Dupree JL, Pomicter AD (2009) Myelin, DIGs, and membrane rafts in the central nervous system. Prostaglandins Other Lipid Mediat. doi:10.1016/j.prostaglandins.2009.04.005

Fozo EM, Quivey RG Jr (2004) Shifts in the membrane fatty acid profile of Streptococcus mutans enhance survival in acidic environments. Appl Environ Microbiol 70:929–936

Fozo EM, Kajfasz JK, Quivey RG Jr (2004) Low pH-induced membrane fatty acid alterations in oral bacteria. FEMS Microbiol Lett 238:291–295

Fulford AJ, Peel WE (1980) Lateral pressures in biomembranes estimated from the dynamics of fluorescent probes. Biochim Biophys Acta 598:237–246

Fullekrug J, Simons K (2004) Lipid rafts and apical membrane traffic. Ann N Y Acad Sci 1014:164–169

Glass RL (1971) Alcoholysis, saponification and the preparation of fatty acid methyl esters. Lipids 6:919–926

Goni FM, Alonso A, Bagatolli LA, Brown RE, Marsh D, Prieto M, Thewalt JL (2008) Phase diagrams of lipid mixtures relevant to the study of membrane rafts. Biochim Biophys Acta 1781:665–684

Gurr M, Harwood JL, Frayn KN (2002) Lipid biochemistry: an introduction. Wiley-Blackwell, New York

Hazel JR (1995) Thermal adaptation in biological membranes—is homeoviscous adaptation the explanation. Annu Rev Physiol 57:19–42

Herman P, Konopasek I, Plasek J, Svobodova J (1994) Time-resolved polarized fluorescence studies of the temperature adaptation in *Bacillus subtilis* using DPH and TMA-DPH fluorescent probes. Biochim Biophys Acta 1190:1–8

Herman P, Konopasek I, Vecer J, Svobodova J (1998) Time-resolved fluorescence and thermal adaptation of *Bacillus subtilis*: the role of membrane proteins. In: Slavik J (ed) Fluorescence microscopy and fluorescent probes. Springer, New York, pp 25–29

Jahnig F (1979) Structural order of lipids and proteins in membranes: evaluation of fluorescence anisotropy data. Proc Natl Acad Sci USA 76:6361–6365

Jordan KN, Oxford L, O'Byrne CP (1999) Survival of low-pH stress by *Escherichia coli* O157:H7: correlation between alterations in the cell envelope and increased acid tolerance. Appl Environ Microbiol 65:3048–3055

Kaneda T (1977) Fatty acids of the genus *Bacillus*: an example of branched-chain preference. Bacteriol Rev 41:391–418

Kaneda T (1991) Iso- and anteiso-fatty acids in bacteria: biosynthesis, function, and taxonomic significance. Microbiol Rev 55:288–302

Kinosita KJ, Kawato S, Ikegami A (1977) A theory of fluorescence polarization decay in membranes. Biophys J 20:289–305

Knutson JR, Beechem JM, Brand L (1983) Simultaneous analysis of multiple fluorescence decay curves—a global approach. Chem Phys Lett 102:501–507

Lakowicz JR (1999) Principles of fluorescence spectroscopy, 2nd edn. Kluwer Academic/Plenum, New York

Lipari G, Szabo A (1980) Effect of librational motion on fluorescence depolarization and nuclear magnetic-resonance relaxation in macromolecules and membranes. Biophys J 30:489–506

Mansilla MC, Cybulski LE, Albanesi D, de Mendoza D (2004) Control of membrane lipid fluidity by molecular thermosensors. J Bacteriol 186:6681–6688

McElhaney RN, Souza KA (1976) Relationship between environmental-temperature, cell-growth and fluidity and physical state of membrane lipids in *Bacillus stearothermophilus*. Biochim Biophys Acta 443:348–359

Mykytczuk NC, Trevors JT, Leduc LG, Ferroni GD (2007) Fluorescence polarization in studies of bacterial cytoplasmic membrane fluidity under environmental stress. Prog Biophys Mol Biol 95:60–82

Owicki JC, Springgate MW, McConnell HM (1978) Theoretical study of protein–lipid interactions in bilayer membranes. Proc Natl Acad Sci USA 75:1616–1619

Poolman B, Blount P, Folgering JH, Friesen RH, Moe PC, van der Heide T (2002) How do membrane proteins sense water stress? Mol Microbiol 44:889–902

Poolman B, Spitzer JJ, Wood JM (2004) Bacterial osmosensing: roles of membrane structure and electrostatics in lipid–protein and protein–protein interactions. Biochim Biophys Acta 1666:88–104

Radin NS (1981) Extraction of tissue lipids with a solvent of low toxicity. Methods Enzymol 72:5–7

Shinitzky M, Barenholz Y (1978) Fluidity parameters of lipid regions determined by fluorescence polarization. Biochim Biophys Acta 515:367–394

Suutari M, Laakso S (1992) Unsaturated and branched chain-fatty acids in temperature adaptation of *Bacillus subtilis* and *Bacillus megaterium*. Biochim Biophys Acta 1126:119–124

Svobodova J, Julak J, Pilar J, Svoboda P (1988) Membrane fluidity in *Bacillus subtilis*. Validity of homeoviscous adaptation. Folia Microbiol (Praha) 33:170–177

Tao T (1969) Time-dependent fluorescence depolarization and brownian rotational diffusion coefficients of macromolecules. Biopolymers 8:609–632

Trevors JT (2003) Fluorescent probes for bacterial cytoplasmic membrane research. J Biochem Biophys Methods 57:87–103

van de Vossenberg JLCM, Driessen AJM, da Costa MS, Konings WN (1999a) Homeostasis of the membrane proton permeability in *Bacillus subtilis* grown at different temperatures. Biochim Biophys Acta Biomembr 1419:97–104

van de Vossenberg JLCM, Driessen AJM, Grant WD, Konings WN (1999b) Lipid membranes from halophilic and alkali-halophilic Archaea have a low H^+ and Na^+ permeability at high salt concentration. Extremophiles 3:253–257

van der Meer W, Pottel H, Herreman W, Ameloot M, Hendrickx H, Schroder H (1984) Effect of orientational order on the decay of the fluorescence anisotropy in membrane suspensions. A new approximate solution of the rotational diffusion equation. Biophys J 46:515–523

van Schaik W, Gahan CG, Hill C (1999) Acid-adapted *Listeria monocytogenes* displays enhanced tolerance against the lantibiotics nisin and lacticin 3147. J Food Prot 62:536–539

Wan FY, Wang YN, Zhang GJ (2002) Influence of the physical states of membrane surface area and center area on lysosomal proton permeability. Arch Biochem Biophys 404:285–292

Yuk HG, Marshall DL (2004) Adaptation of *Escherichia coli* O157:H7 to pH alters membrane lipid composition, verotoxin secretion, and resistance to simulated gastric fluid acid. Appl Environ Microbiol 70:3500–3505

Yuk HG, Marshall DL (2005) Influence of acetic, citric, and lactic acids on *Escherichia coli* O157:H7 membrane lipid composition, Verotoxin secretion, and acid resistance in simulated gastric fluid. J Food Protect 68:673–679

Zannoni C (1981) A theory of fluorescence depolarization in membranes. Mol Physics 42:1303–1320

Zhang GJ, Liu HW, Yang L, Zhong YG, Zheng YZ (2000) Influence of membrane physical state on the lysosomal proton permeability. J Membr Biol 175:53–62